

# Solid-State $^{199}\text{Hg}$ MAS NMR and Vibrational Spectroscopic Studies of Dimercury(I) Compounds

Graham A. Bowmaker,<sup>\*,†</sup> Robin K. Harris,<sup>‡</sup> and David C. Apperley<sup>‡</sup>

Departments of Chemistry, University of Auckland, Private Bag 92019, Auckland, New Zealand, and University of Durham, South Road, Durham DH1 3LE, United Kingdom

Received March 10, 1999

The solid-state  $^{199}\text{Hg}$  MAS NMR spectra of  $\text{Hg}_2\text{X}_2$  ( $\text{X} = \text{Cl}, \text{SCN}, \text{NCO}, \text{CH}_3\text{CO}_2, \text{CF}_3\text{CO}_2$ ) have been measured, and the infrared and Raman spectra of these compounds have been recorded and analyzed to further characterize them and to assist in the interpretation of the NMR data. Spinning-sideband analysis has been used to determine the  $^{199}\text{Hg}$  shielding anisotropy and asymmetry parameters  $\Delta\sigma$  and  $\eta$  from the solid-state  $^{199}\text{Hg}$  MAS NMR spectra. In contrast to the case of the corresponding mercury(II) compounds, the shielding anisotropy is found to be relatively insensitive to the nature of the X group. This is consistent with the view that the electronic environment of the Hg atom in the mercury(I) compounds is dominated by the Hg–Hg bond. The changes in the  $^{199}\text{Hg}$  shielding parameters from the mercury(II) to the corresponding mercury(I) compounds, as well as the changes in these parameters in the mercury(I) compounds with changes in X, can be interpreted in terms of variations in the local paramagnetic contribution to the shielding tensor.

## Introduction

With the recent developments that have taken place in high-resolution NMR techniques for solids,<sup>1–10</sup> there has been increasing interest in the solid-state NMR spectra of heavy-metal nuclei.<sup>4,5</sup> Until recently, there were very few solid-state NMR studies involving  $^{199}\text{Hg}$ , but in the past few years, there has been a considerable increase in the number of such investigations.<sup>4,5,11–22</sup> A recent review of this topic showed that very nearly all of these studies involved compounds of mercury-

(II), the most common oxidation state of mercury in its compounds.<sup>22</sup> There are, however, a number of mercury compounds involving oxidation states lower than (+II), the most common of which are those involving mercury(I).<sup>23–25</sup> All known mercury(I) compounds contain the dimeric mercurous unit  $\text{Hg}_2^{2+}$ , and these compounds are notable for being among the earliest characterized examples of discrete metal–metal bonded species.<sup>25</sup> They are generally two-coordinate, forming linear or near-linear species of the type  $\text{X–Hg–Hg–X}$  or  $[\text{L–Hg–Hg–L}]^{2+}$ . The results of earlier studies suggested a dependence of the Hg–Hg bond length on the nature of the axially bound ligand ( $\text{X}^-$  or  $\text{L}$ ),<sup>26</sup> but results from subsequent single-crystal X-ray studies have shown Hg–Hg distances in the narrow range 2.48–2.54 Å, with no obvious correlation between this parameter and the electronic properties of the ligands.<sup>25,26</sup> A simple view of the bonding in these systems is that the Hg–Hg bond is formed predominantly by overlap of the mercury 6s orbitals and that the ligands form dative bonds via the Hg 6p orbitals.<sup>19</sup> According to this view, the Hg–Hg bonding would contribute only to the diamagnetic shielding, whereas the metal–ligand bonding would contribute to the paramagnetic shielding of the Hg nucleus, so that a study of the  $^{199}\text{Hg}$  shielding tensor for a variety of dimercury(I)

\* Corresponding author. Phone: 64-9-373-7599. Fax: 64-9-373-7422. E-mail: ga.bowmaker@auckland.ac.nz.

<sup>†</sup> University of Auckland.

<sup>‡</sup> University of Durham.

- (1) Haerberlen, U. *Adv. Magn. Reson., Suppl 1* 1976.
- (2) Fyfe, C. A. *Solid State NMR for Chemists*; CFC Press: Guelph, Canada, 1983.
- (3) Harris, R. K. *Nuclear Magnetic Resonance Spectroscopy*; Longman: Harlow, U.K., 1986.
- (4) Davies, J. A.; Dutremez, S. *Coord. Chem. Rev.* 1992, 114, 201.
- (5) Sebal, A. *NMR* 1994, 31, 91.
- (6) Harris, R. K.; Jackson, P.; Merwin, L. H.; Say, B. J. *J. Chem. Soc., Faraday Trans. 1* 1988, 84, 3649.
- (7) Harris, R. K. *Chem. Br.* 1993, 601.
- (8) Mehring, M. In *NMR: Basic Principles and Progress*; Diehl, P., Fluck, E., Günther, H., Kosfeld, R., Eds.; Springer-Verlag: Berlin, 1976; Vol. 11.
- (9) Diehl, P., Fluck, E., Günther, H., Kosfeld, R., Seelig, J., Eds. *NMR: Basic Principles and Progress*; Springer-Verlag: Berlin, 1994; Vols. 30–33.
- (10) Stejskal, E. O.; Memory, J. D. *High Resolution NMR in the Solid State*; Oxford University Press: Oxford, U.K., 1994.
- (11) Wright, J. G.; Natan, M. J.; MacDonnell, F. M.; Ralston, D. M.; O'Halloran, T. V. *Prog. Inorg. Chem.* 1990, 38, 323.
- (12) Harris, R. K.; Sebal, A. *Magn. Reson. Chem.* 1987, 25, 1058.
- (13) Ambrosius, F.; Klaus, E.; Schaller, T.; Sebal, A. *Z. Naturforsch., A* 1995, 50, 423.
- (14) Natan, M. J.; Millikan, C. F.; Wright, J. G.; O'Halloran, T. V. *J. Am. Chem. Soc.* 1990, 112, 3255.
- (15) Santos, R. A.; Gruff, E. S.; Koch, S. A.; Harbison, G. S. *J. Am. Chem. Soc.* 1991, 113, 469.
- (16) Han, M.; Peerson, O. B.; Bryson, J. W.; O'Halloran, T. V.; Smith, S. O. *Inorg. Chem.* 1995, 34, 1187.
- (17) Bowmaker, G. A.; Dance, I. G.; Harris, R. K.; Henderson, W.; Laban, I.; Scudder, M.; Oh, S.-W. *J. Chem. Soc., Dalton Trans.* 1996, 2381.

- (18) Eichele, K.; Kroeker, S.; Wu, G.; Wasylishen, R. E. *Solid State Nucl. Magn. Reson.* 1995, 4, 295.
- (19) Santos, R. A.; Harbison, G. S. *J. Am. Chem. Soc.* 1994, 116, 3075.
- (20) Bowmaker, G. A.; Churakov, A. V.; Harris, R. K.; Oh, S.-W. *J. Organomet. Chem.* 1998, 550, 89.
- (21) Bowmaker, G. A.; Churakov, A. V.; Harris, R. K.; Howard, J. A. K.; Apperley, D. C. *Inorg. Chem.* 1998, 37, 1734.
- (22) Bowmaker, G. A.; Harris, R. K.; Oh, S.-W. *Coord. Chem. Rev.* 1997, 167, 49.
- (23) Aylett, B. J. In *Comprehensive Inorganic Chemistry*; Trotman-Dickenson, A. F., Ed.; Pergamon: Oxford, U.K., 1973; Vol. 3, p 288.
- (24) Brodersen, K.; Hummel, H.-U. In *Comprehensive Coordination Chemistry*; Wilkinson, G., Ed.; Pergamon: Oxford, 1987; Vol. 5, p 1047.
- (25) Taylor, M. J. *Metal-to-Metal Bonded States of the Main Group Elements*; Academic Press: London, 1975; p 17.
- (26) Dorm, E. *J. Chem. Soc., Chem. Commun.* 1971, 466.

complexes should yield information about the bonding in these systems, some aspects of which are still only poorly understood.<sup>27</sup>

To date, there has been only one report on the Hg shielding tensor in a mercury(I) compound. This involved a static single-crystal <sup>199</sup>Hg NMR study of mercury(I) nitrate dihydrate, and the tensor components were analyzed in terms of the simple bonding model described above, involving predominantly 6s–6s overlap for the Hg–Hg bonds and bonding of the two H<sub>2</sub>O ligands with the Hg 6p orbitals.<sup>19</sup> This is not consistent with the view that the Hg atoms in linear mercury(I) compounds use sp hybrid orbitals, analogous to the generally accepted situation in linear mercury(II) complexes.<sup>25,27</sup> Also, in the analysis of these results, the presence of occupied metal–ligand  $\pi$  and  $\pi^*$  orbitals was assumed, but molecular orbital calculations show that  $\pi$  contributions to the bonding in mercury(I) compounds are rather insignificant.<sup>27</sup> If, as is proposed in the above model,<sup>19</sup> the Hg shielding tensor is dominated by contributions from the metal–ligand bonding, this tensor should show a significant dependence on the nature of the axial ligand, as has been found in the case of linear mercury(II) compounds.<sup>20,22</sup> In the present study, we have carried out <sup>199</sup>Hg MAS NMR studies of a range of mercury(I) compounds Hg<sub>2</sub>X<sub>2</sub> (X = Cl, SCN, NCO, OAc, tfa; OAc = acetate, tfa = trifluoroacetate) with a view to investigating this point and to providing more information about the bonding in such compounds.

### Experimental Section

**Materials.** Commercial samples of mercury(I) chloride, Hg<sub>2</sub>Cl<sub>2</sub> (RDH), mercury(I) acetate, Hg<sub>2</sub>(OAc)<sub>2</sub> (BDH), and mercury(I) nitrate dihydrate, Hg<sub>2</sub>(NO<sub>3</sub>)<sub>2</sub>·2H<sub>2</sub>O (BDH) were used without further purification.

**Preparation of Compounds. (a) Mercury(I) Thiocyanate, Hg<sub>2</sub>(SCN)<sub>2</sub>.** A solution of potassium thiocyanate (0.78 g, 8.0 mmol) in water (10 mL) was added, with stirring, to a solution of mercurous nitrate (2.24 g, 4.0 mmol) in water (10 mL) acidified with concentrated HNO<sub>3</sub> (0.4 mL). The product separated from the mixture as a fine, grayish-white precipitate, which was collected by vacuum filtration, washed several times with distilled water, and dried in the air. Despite the claim that the product obtained by this method is light sensitive,<sup>23,28</sup> the compound appears to be stable indefinitely under ambient conditions.

**(b) Mercury(I) Cyanate, Hg<sub>2</sub>(NCO)<sub>2</sub>.** A solution of potassium cyanate (1.2 g, 14.8 mmol) in water (10 mL) was added, with stirring, to a solution of mercurous nitrate (2.8 g, 5 mmol) in water (10 mL) acidified with concentrated HNO<sub>3</sub> (0.5 mL). The product separated from the mixture as a fine, grayish-white precipitate, which was collected by vacuum filtration, washed several times with distilled water, and dried in the air. Anal. Calcd for C<sub>2</sub>Hg<sub>2</sub>N<sub>2</sub>O<sub>2</sub>: C, 4.95; H, 0.0; N, 5.77. Found: C, 4.8; H, 0.0; N, 5.6. The compound gradually turns a darker gray upon standing under ambient conditions over a period of several months.

**(c) Mercury(I) Trifluoroacetate, Hg<sub>2</sub>(tfa)<sub>2</sub>.** This was prepared as a white crystalline solid by a literature method.<sup>29</sup>

**Spectroscopy.** Carbon-13 and mercury-199 magic-angle-spinning spectra were obtained at 75.43 and 53.65 MHz, respectively, using a Varian Unity Plus 300 spectrometer. A 7.0 mm o.d. silicon nitride rotor with Vespel end-caps was used for all spectra, with spin rates in the range 8–11 kHz. Although measurements were nominally made at ambient probe temperature (ca. 25 °C), it is likely that the fast spinning used for the <sup>199</sup>Hg spectra resulted in substantially elevated temperatures (ca. 45 °C).<sup>30</sup> The carbon-13 spectra were recorded with direct

polarization (sometimes referred to as single-pulse excitation). A recycle delay of 5 s was used, and 15 000 transients were collected (100 transients in the case of the acetate). Mercury-199 spectra were recorded with direct polarization (1  $\mu$ s 12° pulses as judged via cross polarization for a sample of [Hg(dmsO)<sub>6</sub>][O<sub>3</sub>SCF<sub>3</sub>]<sub>2</sub>). Centerband signals were located by varying the spinning rate. Recycle delays of 3 s with ca. 20 000 transients were required to obtain acceptable spectra. Spinning-sideband intensities were analyzed to yield values of the shielding tensor components by an iterative computer program written in house.<sup>31</sup> The fitting procedure used a minimum of 13 sidebands plus the centerband and was carried out for spinning rates in the range 8000–11 000 Hz. Accuracy was limited by the high noise levels and by the fact that the spectra required baseline correction. Errors in the shielding tensor parameters were calculated by a published method.<sup>32</sup> These are statistical in nature and may underestimate the true errors, which would also have systematic and experimental reproducibility contributions. The principal components  $\sigma_{11}$ ,  $\sigma_{22}$ , and  $\sigma_{33}$  of the <sup>199</sup>Hg shielding tensor are defined such that

$$|\sigma_{33} - \sigma_{\text{iso}}| \geq |\sigma_{11} - \sigma_{\text{iso}}| \geq |\sigma_{22} - \sigma_{\text{iso}}| \quad (1)$$

where  $\sigma_{\text{iso}}$  is the isotropic, or scalar, shielding constant, related to the principal components of the shielding tensor by

$$\sigma_{\text{iso}} = (1/3)(\sigma_{11} + \sigma_{22} + \sigma_{33}) \quad (2)$$

and measured as

$$\sigma_{\text{iso}} - \sigma_{\text{r}} = -\delta_{\text{iso}} \quad (3)$$

where  $\delta_{\text{iso}}$  is the isotropic chemical shift (the centerband shift) and  $\sigma_{\text{r}}$  is the shielding constant for the reference compound. Chemical shifts were referenced using replacement samples of adamantane ( $\delta_{\text{C}} = 38.4$  ppm for the CH<sub>2</sub> carbon on the tetramethylsilane scale) and [Hg(dmsO)<sub>6</sub>][O<sub>3</sub>SCF<sub>3</sub>]<sub>2</sub> ( $\delta_{\text{Hg}} = -2313$  ppm<sup>33</sup> on the dimethylmercury scale).

Infrared spectra were recorded with 4 cm<sup>-1</sup> resolution at room temperature as Nujol mulls between KBr plates on a Perkin-Elmer Spectrum 1000 Fourier transform infrared spectrometer. Far-infrared spectra were recorded with 2 cm<sup>-1</sup> resolution at room temperature as pressed polythene disks on a Digilab FTS-60 Fourier transform infrared spectrometer employing an FTS-60V vacuum optical bench with a 5 line/mm wire mesh beam splitter, a mercury lamp source, and a pyroelectric triglycine sulfate detector. Raman spectra were recorded at 4.5 cm<sup>-1</sup> resolution using a Jobin-Yvon U1000 spectrometer equipped with a cooled photomultiplier (RCA C31034A) detector. The 514.5 nm exciting line from a Spectra-Physics model 2016 argon ion laser was used.

### Results and Discussion

**Vibrational Spectroscopy.** Little is known about the properties of the mercury(I) pseudohalides Hg<sub>2</sub>(SCN)<sub>2</sub> and Hg<sub>2</sub>(NCO)<sub>2</sub>.<sup>23–25</sup> We have therefore recorded the infrared and Raman spectra of these compounds to obtain information about their structures. The low-wavenumber vibrational spectra are shown in Figures 1 and 2, and the band assignments for all of the fundamental vibrational modes are given in Table 1. A comparison of selected vibrational frequencies for HgX<sub>2</sub><sup>34–36</sup> and Hg<sub>2</sub>X<sub>2</sub><sup>25,36</sup> is given in Table 2.

(30) Bjorholm, T.; Jakobsen, H. J. *J. Magn. Reson.* **1989**, *84*, 204.

(31) (a) Ascenso, J. R.; Bai, H.; Harris, R. K. Unpublished results. (b) Harris, R. K.; Merwin, L. H.; Hagele, G. J. *Chem. Soc., Faraday Trans. 1* **1989**, *85*, 1409.

(32) Olivieri, A. C. *J. Magn. Reson., Ser. A* **1996**, *123*, 207.

(33) Hook, J. M.; Dean, P. A. W.; van Gorkom, L. C. M. *Magn. Reson. Chem.* **1995**, *33*, 77.

(34) Adams, D. M.; Appleby, R. J. *Chem. Soc., Dalton Trans.* **1977**, 1530.

(35) Cooney, R. P.; Hall, J. R. *Aust. J. Chem.* **1969**, *22*, 2117.

(36) Cooney, R. P.; Hall, J. R. *J. Inorg. Nucl. Chem.* **1972**, *34*, 1519.

(27) Schwerdtfeger, P.; Boyd, P. D. W.; Brienne, S.; McFeaters, J. S.; Dolg, M.; Liao, M.-S.; Schwarz, W. H. E. *Inorg. Chim. Acta* **1993**, *213*, 233.

(28) Brauer, G. *Handbuch der Präparativen Anorganischen Chemie*; Enke Verlag: Stuttgart, Germany, 1960.

(29) Sikirica, M.; Grdenic, D. *Acta Crystallogr., Sect. B* **1974**, *30*, 144.

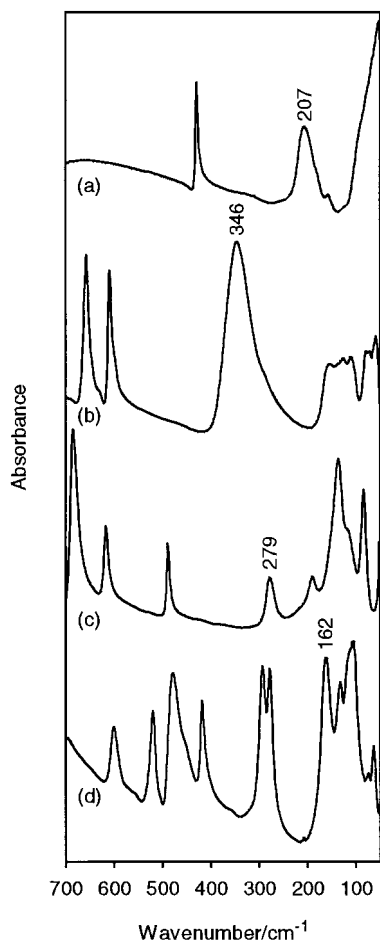


**Figure 1.** Far-IR spectra of  $\text{Hg}_2\text{X}_2$ : (a) X = SCN; (b) X = NCO; (c) X = OAc; (d) X = tfa. Bands assigned to  $\nu(\text{HgX})$  are labeled with their wavenumbers.

The positions of the  $\nu(\text{CN})$ ,  $\nu(\text{CS})$ , and  $\delta(\text{SCN})$  bands in the vibrational spectra of  $\text{Hg}_2(\text{SCN})_2$  are generally consistent with the presence of terminally S-bound thiocyanate groups.<sup>37</sup> The vibrational spectra are readily interpreted in terms of a linear S–Hg–Hg–S structure, analogous to that of the corresponding halides.<sup>26</sup> In particular, the observation of noncoincident bands in the Raman and IR spectra for the symmetric and antisymmetric Hg–S stretching vibrations,  $\nu_s(\text{HgS})$  and  $\nu_a(\text{HgS})$ , respectively, with  $\nu_s(\text{HgS}) > \nu_a(\text{HgS})$ , follows the pattern observed for the  $\nu(\text{HgX})$  modes in  $\text{Hg}_2\text{X}_2$ ;<sup>25</sup> see the data for X = Cl in Table 2. This is the reverse of the situation  $\nu_s(\text{HgX}) < \nu_a(\text{HgX})$ , which is observed for the corresponding mercury(II) species  $\text{HgX}_2$ , this change being due to coupling of  $\nu_s(\text{HgX})$  with the low-frequency  $\nu(\text{HgHg})$  mode in the mercury(I) species. The  $\nu(\text{HgHg})$  mode in  $\text{Hg}_2(\text{SCN})_2$  is assigned to a strong Raman band at  $158 \text{ cm}^{-1}$ , although a Raman band of medium intensity at  $179 \text{ cm}^{-1}$  may also be due to this mode. Strong splitting of the  $\nu(\text{HgHg})$  band was previously observed for other mercury(I) complexes and was attributed to factor group effects.<sup>25</sup> Other evidence for factor group effects in the Raman spectrum of  $\text{Hg}_2(\text{SCN})_2$  is the presence of two  $\nu(\text{CN})$  bands ( $2131, 2113 \text{ cm}^{-1}$ ) and two  $\nu(\text{HgS})$  bands ( $271, 243 \text{ cm}^{-1}$ ). However, the essential absence of bands that are coincident in the IR and Raman spectra suggests a centrosymmetric structure. The only counterindicator to this conclusion is the possible presence of a very weak IR band at  $157 \text{ cm}^{-1}$ , which is almost coincident with the strong

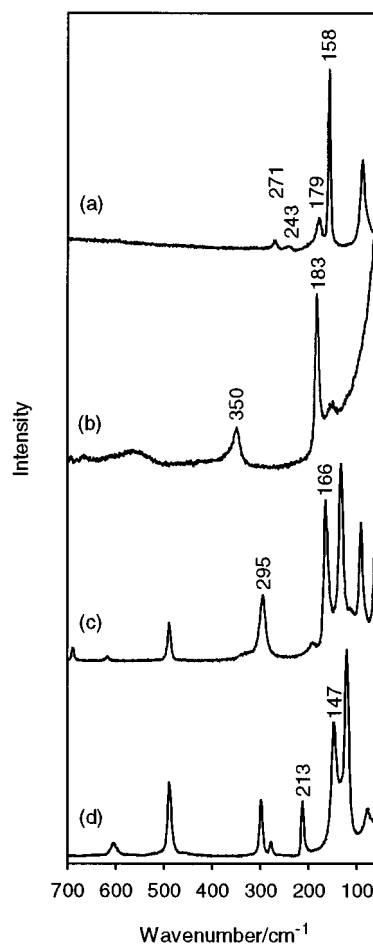


**Figure 2.** Low-wavenumber Raman spectra of  $\text{Hg}_2\text{X}_2$ : (a) X = SCN; (b) X = NCO; (c) X = OAc; (d) X = tfa. Bands assigned to  $\nu(\text{HgX})$  and  $\nu(\text{HgHg})$  are labeled with their wavenumbers.

**Table 1.** Assignments of the Bands ( $\text{cm}^{-1}$ ) in the Vibrational Spectra of  $\text{Hg}_2(\text{SCN})_2$  and  $\text{Hg}_2(\text{NCO})_2$

$\text{Hg}_2(\text{SCN})_2$		$\text{Hg}_2(\text{NCO})_2$		assign <sup>a</sup>
IR	R	IR	R	
2144 vs	2131 m 2113 w	2251 w, sh 2200 vs, sh 2164 vs 2126 s, sh 2077 w, sh	2165 w 2120 w	$\nu(\text{CN})$
884 m	802 w	1378 vw 1353 vw 1291 vw 1266 vw	1356 w 1294 w	$\nu(\text{CE})$
430 s		659 m 611 m	693 vw 668 vw	$\delta(\text{ECN})$
207 s	271 w 243 w 179 m	346 s	565 m, br 350 m	$\nu(\text{HgX})$
157 vw 53 s	158 s 89 s	154 w 138 w, sh 127 w 111 w 79 w 73 w 59 w	183 s 152 m	$\nu(\text{HgHg})?$ $\nu(\text{HgHg})$ $\delta(\text{HgHgX})$
				lattice

<sup>a</sup> E = O or S; X = S or N.

(37) Nakamoto, K. *Infrared and Raman Spectra of Inorganic and Coordination Compounds*, 5th ed.; Wiley: New York, 1997.

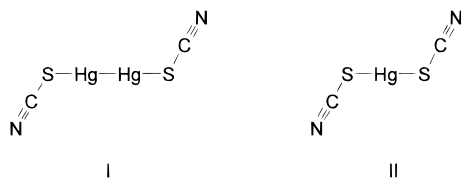
$\nu(\text{HgHg})$  Raman band at  $158 \text{ cm}^{-1}$ . However, on balance, the vibrational spectra generally support a centrosymmetric structure

**Table 2.** Comparison of Selected Vibrational Frequencies ( $\text{cm}^{-1}$ ) for  $\text{HgX}_2$  and  $\text{Hg}_2\text{X}_2$ 

X	$\text{HgX}_2$			ref	$\text{Hg}_2\text{X}_2$				ref
	$\nu_a(\text{HgX})$	$\nu_s(\text{HgX})$	$\delta(\text{XHgX})$		$\nu_a(\text{HgX})$	$\nu_s(\text{HgX})$	$\nu(\text{HgHg})$	$\delta(\text{HgHgX})$	
Cl	370	315	106	34	252	277	167	139, 109	25
SCN	309, 313	270	85	35	207	243, 271	179, 158	89, 53	<i>a</i>
NCO	425	358		<i>b</i>	346	350	183	154–111	<i>a</i>
OAc	314	279		36	279	295	166		36, <i>a</i>
tfa					162	213	147		<i>a</i>

<sup>a</sup> This work. <sup>b</sup> For the  $\text{Hg}(\text{NCO})_2$  units in  $\text{K}_2[\text{Hg}_3(\text{NCO})_8]$ ; ref 21.

which, given the nonlinear M–S–C geometry that normally occurs in S-bonded thiocyanate complexes,<sup>38</sup> would have local  $C_{2h}$  symmetry (structure I). This closely resembles the structure of the corresponding mercury(II) complex (structure II).<sup>39</sup>



The vibrational spectra of the cyanate compound  $\text{Hg}_2(\text{NCO})_2$  are more complex than those of the thiocyanate discussed above, splitting of the bands due to the vibrations of the coordinated NCO groups being observed in both the IR and Raman spectra (see Table 1). It has been claimed that  $\nu(\text{CO})$  increases relative to the free-ion value (ca.  $1250 \text{ cm}^{-1}$ )<sup>37</sup> upon bonding via the N atom,<sup>40</sup> and this is observed in the present complex, with bands due to this mode occurring in the range  $1260\text{--}1380 \text{ cm}^{-1}$ . Neither the structure nor the vibrational spectra of the corresponding mercury(II) compound have been reported to date, but the complex  $\text{K}_2[\text{Hg}_3(\text{NCO})_8]$  has been shown to contain  $\text{Hg}(\text{NCO})_2$  molecules in its lattice, with terminal N-bound cyanate groups and nonlinear  $\text{Hg}\text{--}\text{N}\text{--}\text{C}$  angles of ca.  $130^\circ$ , forming an approximately  $C_{2h}$  structure.<sup>41</sup> The  $\nu(\text{HgN})$  frequencies listed in Table 2 for  $\text{Hg}(\text{NCO})_2$  are those assigned to this species in  $\text{K}_2[\text{Hg}_3(\text{NCO})_8]$ .<sup>21</sup> The presence of the dimercury unit in  $\text{Hg}_2(\text{NCO})_2$  is confirmed by the observation of a strong  $\nu(\text{HgHg})$  band in the Raman spectrum at  $183 \text{ cm}^{-1}$  (Figure 2). This is at the upper end of the range of previously determined  $\nu(\text{HgHg})$  frequencies ( $110\text{--}190 \text{ cm}^{-1}$ )<sup>25</sup> and is comparable to the value of  $185 \text{ cm}^{-1}$  reported for  $\text{Hg}_2\text{F}_2$ .<sup>25</sup> It is also close to the value of  $\nu(\text{HgHg}) = 181 \text{ cm}^{-1}$  reported for the N-bonded mercury(I) complex of *N,N'*-diacetylhydrazine:  $[\text{Hg}_2\text{N}(\text{COCH}_3)_2\text{N}(\text{COCH}_3)]_n$ .<sup>25</sup>

The  $\nu(\text{HgN})$  bands of  $\text{Hg}_2(\text{NCO})_2$  are observed at about  $350 \text{ cm}^{-1}$  (Figures 1 and 2). The IR-active antisymmetric mode,  $\nu_a(\text{HgN})$ , shows a substantial decrease in frequency relative to that of the corresponding mercury(II) complex, and this decrease is similar in magnitude to those observed for  $\text{Hg}_2\text{Cl}_2$  and  $\text{Hg}_2(\text{SCN})_2$  (Table 2). This reflects a substantial weakening of the  $\text{Hg}\text{--}\text{X}$  bond in  $\text{Hg}_2\text{X}_2$  relative to that in  $\text{HgX}_2$ . The frequency of the Raman-active symmetric mode,  $\nu_s(\text{HgN})$ , for  $\text{Hg}_2(\text{NCO})_2$  is almost the same as that of the IR-active antisymmetric mode,  $\nu_a(\text{HgN})$ . For the series  $\text{Hg}_2\text{X}_2$  ( $\text{X} = \text{Cl}, \text{Br}, \text{I}$ ),  $\nu_s(\text{HgX})$  is greater than  $\nu_a(\text{HgX})$  (in contrast to the situation for  $\text{HgX}_2$ ), but the difference between these decreases along this series. The reason for these observations is that the  $\text{Hg}\text{--}\text{X}$  and  $\text{Hg}\text{--}$

$\text{Hg}$  coordinates are strongly coupled, because the  $\nu_s(\text{HgX})$  and  $\nu(\text{HgHg})$  modes have the same symmetry and similar frequencies and the degree of coupling increases as  $\nu_s(\text{HgX})$  decreases. In the  $\text{X} = \text{NCO}$  case,  $\nu_s(\text{HgX})$  is higher than for the halides mentioned above, so that the degree of coupling is reduced to the point where  $\nu_s(\text{HgN})$  is approximately equal to  $\nu_a(\text{HgN})$  (Table 2). This near-coincidence is therefore proposed to be “accidental”, but this and other possible coincidences between the IR and Raman spectra (Table 1) do not allow the definite conclusion of a centrosymmetric structure for the compound. However, the other features of the vibrational spectra discussed above strongly support a structure with a linear or near-linear  $\text{N}\text{--}\text{Hg}\text{--}\text{Hg}\text{--}\text{N}$  arrangement, and it is equally clear that the crystal structure is not isomorphous with that of  $\text{Hg}_2(\text{SCN})_2$ .

The low-wavenumber vibrational spectra of mercury(I) acetate and trifluoroacetate are shown in Figures 1 and 2. The structure of  $\text{Hg}_2(\text{OAc})_2$  has not been reported to date, but that of the trifluoroacetate  $\text{Hg}_2(\text{tfa})_2$  shows the presence of discrete molecules of  $C_2$  symmetry, with monodentate trifluoroacetate groups bound to the dimercury unit to give a near-linear  $\text{O}\text{--}\text{Hg}\text{--}\text{Hg}\text{--}\text{O}$  array with  $\text{Hg}\text{--}\text{Hg}\text{--}\text{O} = 166.6^\circ$ .<sup>42</sup> The vibrational spectra of the acetate complex have been interpreted on the basis of a similar model.<sup>36</sup> The frequencies of the  $\nu(\text{HgO})$  and  $\nu(\text{HgHg})$  modes for these two compounds are given, together with those for the  $\nu(\text{HgO})$  modes of mercury(II) acetate, in Table 2. The present results for  $\text{Hg}_2(\text{OAc})_2$  are essentially in agreement with the previous report, the main difference being the observation of a single  $\nu_a(\text{HgO})$  IR band at  $279 \text{ cm}^{-1}$  (Figure 1), rather than the previously reported doublet at  $268, 283 \text{ cm}^{-1}$ .<sup>36</sup> The occurrence of multiple strong bands below  $200 \text{ cm}^{-1}$  renders the assignment of  $\nu(\text{HgHg})$  less certain than in the case of the halides or pseudohalides; this situation is found for several other mercury(I) complexes with oxygen-donor ligands.<sup>25</sup> In accordance with the previous study of the acetate,<sup>36</sup> we assign the strong band of highest frequency below  $200 \text{ cm}^{-1}$  to  $\nu(\text{HgHg})$  for both compounds (Table 2). The mutual exclusion of the  $\nu(\text{HgO})$  bands between the IR and the Raman spectra (Table 2) implies the presence of a centrosymmetric  $\text{O}\text{--}\text{Hg}\text{--}\text{Hg}\text{--}\text{O}$  arrangement, as is found in the crystal structure of  $\text{Hg}_2(\text{tfa})_2$ .<sup>42</sup>

**Mercury-199 MAS NMR Spectra.** The solid-state <sup>199</sup>Hg MAS NMR spectra of  $\text{Hg}_2\text{Cl}_2$  and  $\text{Hg}_2(\text{OAc})_2$  are shown in Figure 3. As with other mercury complexes that show large <sup>199</sup>Hg shielding anisotropy, the spectra consist of a centerband flanked by a number of spinning sidebands.<sup>22</sup> The chemical shift and shielding parameters obtained from a spinning-sideband analysis of these spectra, and of the spectra of the other compounds studied in this work, are compared with the previously reported data for  $\text{Hg}_2(\text{NO}_3)_2 \cdot 2\text{H}_2\text{O}$ <sup>19</sup> in Table 3. Apart from the spectra of the compounds discussed in the previous section, the spectrum of dimercury(I) sulfate,  $\text{Hg}_2\text{SO}_4$ , was also recorded. This compound has been shown to contain infinite

(38) Vrieze, K.; van Koten, G. In *Comprehensive Coordination Chemistry*; Wilkinson, G., Ed.; Pergamon: Oxford, U.K., 1987; Vol. 2, p 225.

(39) Beauchamp, A. L.; Goutier, D. *Can. J. Chem.* **1972**, *50*, 977.

(40) Ellestad, O. H.; Klæboe, P.; Tucker, E. E.; Songstad, J. *Acta Chem. Scand.* **1972**, *26*, 3579.

(41) Thiele, G.; Hilfrich, P. Z. *Naturforsch.*, **B 1978**, *33*, 597.

(42) Sikirica, M.; Grdenic, D. *Acta Crystallogr., Sect. B* **1974**, *30*, 144.

**Table 3.**  $^{199}\text{Hg}$  Chemical Shifts and Shielding Tensor Parameters from Solid-State  $^{199}\text{Hg}$  NMR Spectra

compound	$\sigma_{11} - \sigma_r/\text{ppm}$	$\sigma_{22} - \sigma_r/\text{ppm}$	$\sigma_{33} - \sigma_r/\text{ppm}$	$\delta_{\text{iso}}/\text{ppm}$	$\Delta\sigma/\text{ppm}$	$\eta$	ref
$\text{Hg}_2\text{Cl}_2$	-396(39)	-53(36)	3598(39)	-1050	3822(58)	0.14(3)	<i>a</i>
$\text{Hg}_2(\text{SCN})_2$	-157(30)	219(25)	2988(37)	-1017	2957(56)	0.19(2)	<i>a</i>
$\text{Hg}_2(\text{NCO})_2$	-498(54)	10(43)	3735(75)	-1082	3979(112)	0.19(2)	<i>a</i>
$\text{Hg}_2(\text{OAc})_2$	326(57)	326(57)	3699(20)	-1450	3374(30)	0.00(5)	<i>a</i>
$\text{Hg}_2(\text{tfa})_2$	507(38)	508(38)	3931(13)	-1649	3423(20)	0.00(3)	<i>a</i>
$\text{Hg}_2\text{SO}_4$	505(87)	606(87)	3544(13)	-1552	2988(34)	0.05(9)	<i>a</i>
$\text{Hg}_2(\text{NO}_3)_2 \cdot 2\text{H}_2\text{O}^b$	435.2	496.7	3669.3	-1533.7	3203	0.03	19
$\text{HgCl}_2$	282(27)	573(26)	4019(26)	-1625	3592(37)	0.12(2)	20
$\text{Hg}(\text{SCN})_2$	81(23)	428(21)	3390(24)	-1300	3135(37)	0.17(2)	21
$\text{Hg}(\text{OAc})_2$	1859	1947	3685	-2497	1782	0.07	18

<sup>a</sup> This work. <sup>b</sup> Static single-crystal measurement.

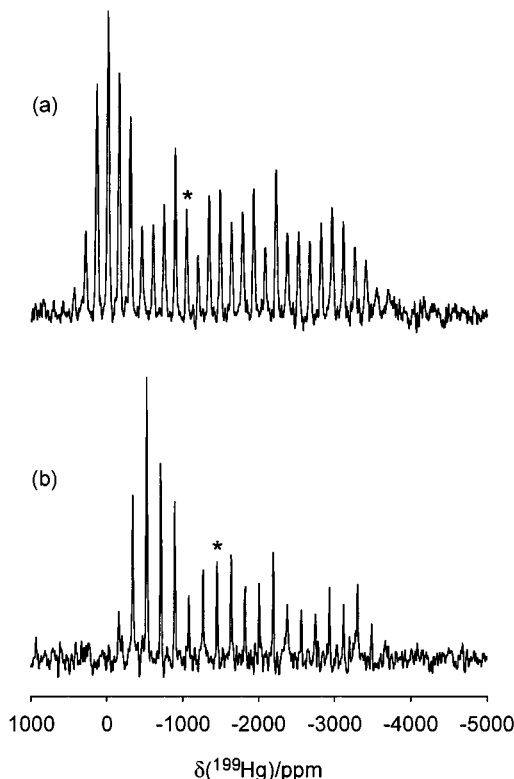


**Figure 3.** 53.6 MHz  $^{199}\text{Hg}$  MAS NMR spectra of (a)  $\text{Hg}_2\text{Cl}_2$  (spinning rate  $\nu_s = 8000$  Hz) and (b)  $\text{Hg}_2(\text{OAc})_2$  ( $\nu_s = 10000$  Hz). Baseline corrections and line broadening (500 Hz) were applied prior to plotting. The centerband is indicated by the asterisk.

— $\text{SO}_4$ — $\text{Hg}$ — $\text{Hg}$ — $\text{SO}_4$ — $\text{Hg}$ — $\text{Hg}$ — chains with a nearly linear  $\text{Hg}$ — $\text{Hg}$ — $\text{O}$  angle of  $164.9^\circ$ .<sup>43</sup> The spectrum of  $\text{Hg}_2(\text{NCO})_2$  was of significantly poorer quality than those of the other dimercury(I) compounds in Table 3, and this accounts for the somewhat greater errors in the shielding parameters for this compound. An attempt to record the spectrum of dimercury(I) *o*-phthalate,  $\text{Hg}_2(\text{OOC})_2\text{C}_6\text{H}_4$ , resulted in a spectrum that was not of sufficient quality to allow analysis. Of all the compounds examined, this is the only one for which the two Hg atoms in the dimercury(I) unit are inequivalent.<sup>44</sup> An attempt was also made to record the spectrum of dimercury(I) dibromide,  $\text{Hg}_2\text{Br}_2$ . As in the case of the corresponding mercury(II) compound  $\text{HgBr}_2$ ,<sup>20</sup> this was unsuccessful. A possible reason for this is that unresolved coupling to the  $^{79}\text{Br}$ ,  $^{81}\text{Br}$  nuclei causes severe broadening of the  $^{199}\text{Hg}$  signals. A similar effect is probably responsible for the significantly greater line width in the  $^{199}\text{Hg}$  spectrum of  $\text{Hg}_2\text{Cl}_2$  compared with that of  $\text{Hg}_2(\text{OAc})_2$  (Figure

3). The greater magnetic and quadrupole moments of  $^{79}\text{Br}$ ,  $^{81}\text{Br}$  relative to  $^{35}\text{Cl}$ ,  $^{37}\text{Cl}$  would result in still broader lines for  $\text{Hg}_2\text{Br}_2$ .

The shielding anisotropy is defined as

$$\Delta\sigma = \sigma_{33} - \frac{1}{2}(\sigma_{11} + \sigma_{22}) \quad (4)$$

and the departure of the shielding tensor from axial symmetry is described by the asymmetry parameter

$$\eta = (\sigma_{22} - \sigma_{11})/(\sigma_{33} - \sigma_{\text{iso}}) \quad (5)$$

We recently showed that anisotropic  $^{199}\text{Hg}$  shielding parameters can be interpreted on the basis of the expressions which have been derived for the local paramagnetic contribution to the shielding.<sup>22</sup> Within the average excitation energy (AEE) approximation, the expressions for the principal components of the local paramagnetic shielding tensor, for the case where the shielding is due to electron density in the valence p orbitals only and the local symmetry is sufficiently high that cross terms in the charge density matrix are zero, are

$$\sigma_{xx} = (n_y + n_z - n_y n_z)\sigma_p \quad (6)$$

$$\sigma_{yy} = (n_x + n_z - n_x n_z)\sigma_p \quad (7)$$

$$\sigma_{zz} = (n_x + n_y - n_x n_y)\sigma_p \quad (8)$$

where  $n_x$ ,  $n_y$ ,  $n_z$  are the populations of the Hg  $6p_x$ ,  $6p_y$ ,  $6p_z$  orbitals, respectively, and  $\sigma_p$  is a constant relating to the contribution of the valence  $np$  orbitals to the shielding:

$$\sigma_p = -\mu_0 e^2 \langle r^{-3} \rangle_{np} / 4\pi m^2 \Delta E \quad (9)$$

Here  $\mu_0$  is the permeability constant,  $e$  is the electronic charge,  $m$  is the electron rest mass,  $\Delta E$  is the average excitation energy, and  $\langle r^{-3} \rangle_{np}$  is the expectation value of  $r^{-3}$  for the valence  $np$  electron.<sup>45,46</sup> The average, or isotropic, local paramagnetic shielding derived from the above is

$$\sigma_{\text{iso}} = (1/3)[2n_x + 2n_y + 2n_z - n_x n_y - n_y n_z - n_x n_z]\sigma_p \quad (10)$$

In both  $\text{HgX}_2$  and  $\text{Hg}_2\text{X}_2$ , the Hg atoms are involved in  $\sigma$ -bonding, which mainly concerns the Hg  $6s$  and  $6p_z$  orbitals (the  $z$  axis lies along the linear axis of the molecules). Thus, the only nonzero orbital population in eqs 6–8 is the Hg  $6p_z$  population  $n_z$  ( $=n$ ). This yields  $\sigma_{xx} = \sigma_{yy} = n\sigma_p$ ;  $\sigma_{zz} = 0$ . Since  $\sigma_p$  is negative (eq 9), this yields  $\sigma_{zz} > \sigma_{xx} = \sigma_{yy}$ . If it is assumed

(43) Dorm, E. *Acta Chem. Scand.* **1969**, *23*, 1607.

(44) Lindh, B. *Acta Chem. Scand.* **1967**, *21*, 2743.

(45) Webb, G. A. Factors Contributing to the Observed Chemical Shifts of Heavy Nuclei. In *NMR of Newly Accessible Nuclei*; Laszlo, P., Ed.; Academic Press: New York, 1983; Vol. 1, p 79.

(46) Jameson, C. J.; Gutowsky, H. S. *J. Chem. Phys.* **1964**, *40*, 1714.

that the diamagnetic contributions to the shielding are isotropic, and so contribute equally to all three principal components of the shielding tensor, the above relationship should also hold for the total shielding constants. Defining the principal axes of the shielding tensor according to eq 1 yields the relationship  $\sigma_{33} > \sigma_{11} = \sigma_{22}$ . Inspection of the results for  $\text{HgX}_2$  and  $\text{Hg}_2\text{X}_2$  in Table 3 shows that the experimental values correspond closely to this relationship; the small deviations from equality of  $\sigma_{11}$  and  $\sigma_{22}$  in the solid-state data are due to small deviations from axial symmetry in the primary and/or secondary bonding interactions. Substitution of the above expressions for the shielding tensor components for linear  $\text{HgX}_2$  into eq 4 yields  $\Delta\sigma = -n\sigma_p$ . Since  $\sigma_p$  is negative (eq 9),  $\Delta\sigma$  is positive. Thus  $\Delta\sigma$  is proportional to the  $6p_z$  population  $n$  which, in turn, is proportional to the  $\sigma$ -donor strength of the ligand, and so a strong  $\sigma$ -donor ligand, such as  $\text{Cl}^-$ , will result in a greater  $n$  than will a weaker  $\sigma$ -donor, such as  $\text{OAc}^-$ . Therefore  $\Delta\sigma$  is predicted to be greater for  $\text{HgCl}_2$  than for  $\text{Hg}(\text{OAc})_2$ , and the results in Table 3 show that this prediction is confirmed. The same relationship is observed for the mercury(I) compounds  $\text{Hg}_2\text{Cl}_2$  and  $\text{Hg}_2(\text{OAc})_2$ , but the difference is much smaller than for the corresponding mercury(II) compounds. The shielding anisotropy for  $\text{Hg}_2\text{Cl}_2$  is only slightly greater than that for  $\text{HgCl}_2$ , whereas the value for  $\text{Hg}_2(\text{OAc})_2$  is about twice as great as that for  $\text{Hg}(\text{OAc})_2$ . This result is difficult to reconcile with the previously expressed view that the shielding anisotropy is dominated by the mercury–ligand bonding.<sup>19</sup> If this were the case, then  $\Delta\sigma$  for  $\text{Hg}_2(\text{OAc})_2$  should only be approximately half the value for  $\text{Hg}(\text{OAc})_2$ , since there is only one Hg–O bond for each Hg atom in the former, compared to two in the latter.

A simple explanation for the observed  $\Delta\sigma$  values for the dimercury(I) compounds can be obtained by considering the dimercury(I) compounds to be linear mixed-ligand complexes  $\text{YHgX}$  where Y is the other X–Hg unit in the molecule. For each mercury atom, the Hg  $6p_z$  orbital population consists of contributions from both the Y and X ligands. The Hg orbitals involved in the bonding must have some  $6p_z$  character if the Hg–Hg bonding is to affect the  $6p_z$  orbital populations. This would be the case if the orbitals involved were sp hybrids, as is normally assumed in the case of linear mercury compounds, although it should be recognized that this is a limiting case corresponding to the maximum possible degree of  $6p_z$  orbital involvement. A theoretical study of several mercury compounds yielded equal  $6p_z$  orbital populations of 0.40 for  $\text{HgCl}_2$  and  $\text{Hg}_2\text{Cl}_2$ .<sup>27</sup> According to the model discussed above, this would result in equal  $\Delta\sigma$  values for these two compounds, in good agreement with the experimental observations (Table 3). No calculations have been reported for corresponding carboxylate compounds, but for the fluorides, the  $6p_z$  orbital population increases from 0.24 to 0.31 from  $\text{HgF}_2$  to  $\text{Hg}_2\text{F}_2$ .<sup>27</sup> This indicates that the Hg–Hg bond in the dimercury(I) compound contributes more to the  $6p_z$  orbital population than the Hg–X bond does. If this is the case, then this orbital population should be less sensitive to changes in X than it is in the corresponding mercury(II) compounds. According to the model for the paramagnetic shielding discussed above, this implies that the shielding anisotropy  $\Delta\sigma$  should show a smaller X-dependence for the dimercury(I) compounds, in good agreement with the experimental observations (Table 3). Nevertheless, there is a significant dependence of  $\Delta\sigma$  on X, and this is such that  $\Delta\sigma$  decreases as the  $\sigma$ -donor strength of  $\text{X}^-$  decreases (e.g., from X = Cl to X = OAc). This can also be readily understood in terms of the model discussed above, since the weaker  $\sigma$ -donor donates less electron density to the Hg  $6p_z$  orbital and thus produces a lower

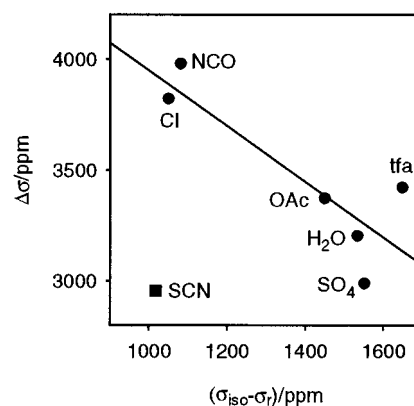


**Figure 4.** Plot of the shielding anisotropy  $\Delta\sigma$  for  $\text{Hg}_2\text{X}_2$  (X = Cl, NCO, OAc, tfa),  $\text{Hg}_2\text{SO}_4$ , and  $\text{Hg}_2(\text{NO}_3)_2 \cdot 2\text{H}_2\text{O}$  (●) and for  $\text{Hg}_2(\text{SCN})_2$  (■) against the corresponding isotropic shielding constant  $\sigma_{\text{iso}} - \sigma_r$ .

shielding anisotropy,  $\Delta\sigma$ . Compared to those for the other  $\text{Hg}_2\text{X}_2$  compounds,  $\Delta\sigma$  for  $\text{Hg}_2(\text{SCN})_2$  is unexpectedly low, and this point will be discussed further below.

The values of the asymmetry parameter  $\eta$  obtained for the mercury(I) compounds (Table 3) are all less than 0.2 (small values of  $\eta$  are difficult to determine accurately),<sup>6,47</sup> implying that the shielding tensor is almost axially symmetric in these compounds. This is as expected for a linear or near-linear X–Hg–Hg–X arrangement such as those observed in the structures of these systems or those deduced from the vibrational spectra (see above).

The isotropic shielding constants are obtained from the centerband shifts  $\delta_{\text{iso}}$  (eq 2), values of which are listed in Table 3 for the compounds studied in the present work. The relationship of this parameter to the electronic structure of the complex is given by eq 10. For the linear  $\text{HgX}_2$  and  $\text{Hg}_2\text{X}_2$  cases, this yields  $\sigma_{\text{iso}} = (2/3)n\sigma_p$ , compared with the corresponding expression derived above for the shielding anisotropy  $\Delta\sigma = -n\sigma_p$ , so that a plot of  $\Delta\sigma$  vs  $\sigma_{\text{iso}}$  should be linear, with a slope of  $-1.5$ . Such a plot for the various  $\text{Hg}_2\text{X}_2$  compounds (excluding X = SCN) in Table 3 is shown in Figure 4. An approximately linear relationship is observed with a slope of  $-1.3 \pm 0.4$ , and the compounds clearly fall into two separate groups: the halides and pseudohalides, with isotropic shieldings ( $\sigma_{\text{iso}} - \sigma_r$ ) of about 1000 ppm, and the oxygen-donor ligands, with isotropic shieldings of about 1500 ppm. The decrease in  $\Delta\sigma$  from the halide to the oxygen-donor ligands has been explained above in terms of the decrease in ligand  $\sigma$ -donor strength. The anomalously low  $\Delta\sigma$  value for  $\text{Hg}_2(\text{SCN})_2$  was also mentioned above, and this results in the point for this compound lying well below the correlation line for the other compounds in Figure 4. Exactly the same kind of anomaly has been observed for the X = SCN compounds in a corresponding plot for  $\text{HgX}_2$  and  $\text{HgX}(\text{OAc})$  and was attributed to the presence of secondary bonding involving intermolecular interactions between the Hg atoms and the N atoms of the SCN groups on neighboring molecules.<sup>20</sup> It is interesting to note that this anomaly does not occur for  $\text{Hg}_2(\text{NCO})_2$ , consistent with the fact that the cyanate group normally bonds via the N atom and not via the O atom.<sup>38</sup>

**Carbon-13 MAS NMR Spectra.** The  $^{13}\text{C}$  MAS NMR parameters for  $\text{Hg}_2\text{X}_2$  (X = SCN, NCO, OAc) are given in Table 4, together with those for  $\text{HgX}_2$  (X = SCN, OAc). The  $^{13}\text{C}$

(47) (a) Hawkes, G. E.; Sales, K. D.; Lian, L. Y.; Gobetto, R. *Proc. R. Soc. London, Ser. A* **1989**, *424*, 93. (b) Clayden, N. J.; Dobson, C. M.; Lian, L.-Y.; Smith, D. J. *J. Magn. Reson.* **1986**, *69*, 476.

**Table 4.** Solid-State  $^{13}\text{C}$  NMR Parameters for Mercury Complexes

complex	carbon	$\delta(^{13}\text{C})/\text{ppm}$	$ ^nJ(^{199}\text{Hg}^{13}\text{C}) /\text{Hz}$	ref
$\text{Hg}(\text{SCN})_2$	SCN	129.4		21
$\text{Hg}_2(\text{SCN})_2$	SCN	129.9		<i>a</i>
$\text{Hg}_2(\text{NCO})_2$	NCO	138.0		<i>a</i>
$\text{Hg}(\text{OAc})_2$	CH <sub>2</sub>	180.9	118 ( $^2J$ )	52
		176.8	156 ( $^2J$ )	
	CH <sub>3</sub>	24.7	176 ( $^3J$ )	
		24.3	195 ( $^3J$ )	
$\text{Hg}_2(\text{OAc})_2$	CH <sub>2</sub>	181.4	<120 ( $^2J$ )	<i>a</i>
	CH <sub>3</sub>	26.1	<150 ( $^3J$ )	

<sup>a</sup> This work.

spectra of  $\text{Hg}(\text{SCN})_2$  and  $\text{Hg}(\text{NCO})_2$  showed single lines, consistent with the proposed structures of these compounds (see Vibrational Spectroscopy section above). The  $^{13}\text{C}$  chemical shift in  $\text{Hg}_2(\text{SCN})_2$  is very similar to that in  $\text{Hg}(\text{SCN})_2$ , showing that the S-bound structure observed for  $\text{Hg}(\text{SCN})_2$ <sup>39</sup> is also present in  $\text{Hg}_2(\text{SCN})_2$ , in agreement with the results from the vibrational spectra discussed above. It has previously been shown that the  $^{13}\text{C}$  chemical shifts of S- and N-bound thiocyanate are lower and higher than the value for ionic thiocyanate (134.0 ppm), respectively.<sup>48,49</sup> The shifts in both of the above complexes conform to this rule but are significantly greater than those in  $[\text{Au}(\text{SCN})_2]^-$  (116.3 ppm) or  $[\text{Hg}(\text{SCN})_4]^{2-}$  (124.8 ppm) and are higher than those observed for a range of other diamagnetic S-bound thiocyanate complexes,<sup>48</sup> while still remaining less than that for ionic thiocyanate. It has been claimed that the  $^{13}\text{C}$  chemical shift of O-bound cyanate lies in the range 104–119 ppm, while that of N-bound cyanate occurs in the range 114–132 ppm.<sup>50,51</sup> The value observed in the present work for  $\text{Hg}_2(\text{NCO})_2$  significantly extends the upper limit of the N-bound range to 138 ppm. The values reported for a number of other N-bound cyanate complexes lie below the value for ionic cyanate (127.9 ppm),<sup>48,50</sup> and  $\text{Hg}_2(\text{NCO})_2$  is an unusual case in which the shift lies above this value.

The  $^{13}\text{C}$  spectrum of  $\text{Hg}_2(\text{OAc})_2$  showed the expected signals due to the acetate ligand, but the long-range ( $^2J$ ,  $^3J$ ) couplings

to  $^{199}\text{Hg}$ , which were observed in  $\text{Hg}(\text{OAc})_2$  (Table 4),<sup>52</sup> were not seen in the dimercury(I) compound. The signals showed a slight additional broadening near the baseline, and from the line widths in this region, the upper limits to the long-range couplings were estimated (Table 4). These are less than the values observed in the mercury(II) complex, which is surprising because a greater Hg 6s population would be expected in the dimercury(I) compound. This must be counteracted by the lower effective charge on the Hg atom and the weaker Hg–O bonding (reflected in the lower  $\nu_a(\text{HgO})$  value) in the dimercury(I) compound. In contrast to the situation for  $\text{Hg}(\text{OAc})_2$ , where separate  $^{13}\text{C}$  signals are seen for the two crystallographically inequivalent acetate groups in the molecule,<sup>12,52</sup> only single lines for each type of carbon atom are seen in the spectrum of  $\text{Hg}_2(\text{OAc})_2$ , which is consistent with the centrosymmetric structure proposed for this compound (see Vibrational Spectroscopy section above).

### Conclusion

The vibrational spectra of  $\text{Hg}_2\text{X}_2$  ( $\text{X} = \text{SCN}, \text{NCO}, \text{OAc}$ ) show that these compounds have structures similar to those of their halide and trifluoroacetate counterparts. In contrast to those for the corresponding mercury(II) compounds, the  $^{199}\text{Hg}$  shielding anisotropies for a range of  $\text{Hg}_2\text{X}_2$  compounds are found to be relatively insensitive to the nature of the X group. This implies that the electronic environment of the Hg atom in the mercury(I) compounds is dominated by the Hg–Hg bond, a view which is consistent with the fact that the Hg–Hg force constants determined from the vibrational frequencies of  $\text{Hg}_2\text{X}_2$  are considerably greater than the Hg–X force constants.<sup>25</sup> A previous conclusion (based on the measured direction of the principal axis of the  $^{199}\text{Hg}$  shielding tensor in  $[\text{Hg}_2(\text{OH})_2]^{2+}$ ) that the shielding tensor is dominated by contributions from metal–ligand bonding<sup>19</sup> is not verified by the results obtained for the greater range of compounds examined in the present study.

**Acknowledgment.** We thank Ms. Catherine Hobbis and Dr. J. Seakins for help with the vibrational spectroscopy. We are grateful to the University of Auckland Research Committee for financial assistance and to the EPSRC for access to the National Solid-State NMR Service, based at Durham.

IC9905648

(48) Kargol, J. A.; Crecey, R. W.; Burmeister, J. L. *Inorg. Chem.* **1979**, *18*, 2532.

(49) Zumbulyadis, N.; Gysling, H. J. *J. Am. Chem. Soc.* **1982**, *104*, 3246.

(50) Coyer, M. J.; Herber, R. H.; Cohen, S. *Inorg. Chim. Acta* **1990**, *175*, 47.

(51) Wehrli, F. W.; Marchand, A. P.; Wehrli, S. *Interpretation of Carbon-13 NMR Spectra*; Wiley: Chichester, U.K., 1988.

(52) Barron, P. F. *J. Organomet. Chem.* **1982**, *236*, 157.